Progress In Electromagnetics Research B, Vol. 58, 111–121, 2014

Printed Egg Curved Slot Antennas for Wideband Applications

Sudhanshu Verma[1, *] and Preetam Kumar[2]

Abstract—This paper presents a novel design of an egg curve based wide-slot antenna for various wideband applications. The proposed printed antenna consists of an egg curved slot with a similar tuning stub. The egg curve is obtained by introducing an egg shaping parameter into standard elliptic curve equation. The effect on the impedance bandwidth through the variations in antenna design parameters has been investigated and analysed in detail. To validate the theoretical design, various egg curved slot antennas were designed, fabricated and measured. Good agreement between the simulated results and the measured ones is observed. An empirical formula is also proposed to approximately determine the frequency corresponding to the lower edge of −10 dB operating bandwidth. The results demonstrate that the proposed egg curved slot antenna (ECSA) can obtain a measured bandwidth (BW) of 164.46% (1.95–20.0 GHz) for $|S_{11}| \leq -10$ dB. A stable realised gain of about 4.1–5.1 dBi with consistent radiation patterns are measured over more than the entire ultrawideband (UWB) bandwidth (3.1–10.6 GHz) which makes it a suitable candidate for wideband and UWB wireless system applications.

1. INTRODUCTION

In recent years, printed slot antennas are under consideration for use in wideband systems due to their attractive merits of wide impedance bandwidth, simple structure, low profile, low cost, light weight, simple to fabricate and their ease of integration with active devices.

Many antenna designers have investigated printed wide-slot antennas. For instance, a printed wide-slot antenna fed by a microstrip line with a rotated slot for bandwidth enhancement is proposed in [1] with operating bandwidth of 2.2 GHz. The bandwidth is further improved to 4.29 GHz in [2] by designing a printed microstrip line-fed rhombus slot antenna with a pair of parasitic strips. An eye shaped antenna is proposed in [3] to achieve a bandwidth of 1.2–4.5 GHz but its gain is reduced significantly from approximately 2 dBi to 0 dBi within the operational band. Similarly, a large gain fluctuation of 6 dBi approximately is observed in printed elliptical monopole antenna with modified feeding structure for bandwidth enhancement [4].

Meanwhile, many antenna researchers have reported their investigation on coplanar waveguide (CPW) fed printed wide-slot antennas. Therefore, several slot geometries are studied for bandwidth enhancement including: square [5], circular [6] and koch fractal [7].

The bandwidth enhancement of the CPW-fed wide-slot antenna mainly depends on the slot and the tuning stub. In [8], CPW-fed E-shaped feed stubs and slots with rounded corners ($85 \times 85\,\text{mm}^2$) are presented with a bandwidth of 2.83–18.2 GHz (more than 146%) for broadband communication systems. In [9], a U-shaped tuning stub is used with circular/elliptical slot to achieve the impedance bandwidth of 110% with gain varying from 1.9–5.1 dBi. It is obvious that the printed wide-slot antenna may achieve a wide bandwidth based on design of various special slots and stubs.

Recently, antenna designers have focused on curve based antenna geometries for bandwidth enhancement as various antenna shapes with different bandwidths may be generated through the

Received 4 January 2014, Accepted 29 January 2014, Scheduled 3 February 2014

* Corresponding author: Sudhanshu Verma (sverma@iitp.ac.in).

[1] Department of Electrical Engineering, Indian Institute of Technology, Patna, Bihar 800013, India. [2] Department of Electrical Engineering, Indian Institute of Technology, Patna, Bihar 800013, India.

variations in parameters of antenna design curve equation. In [10], Ma and Tseng have proposed a pair of curved radiating slots fed by the CPW feedline for ultrawideband applications. In [11], a binomial curve function of order N has been proposed to design planar binomial curved monopole antenna for UWB applications. The patch shape has been varied from triangular ($N = 1$) to rectangular ($N = \infty$) by changing the order N of the binomial curve equation but binomial curved monopole antenna showed little influence over the antenna bandwidth with variation in order N. In [12], using the same binomial curve as in [11], a CPW-fed wideband printed binomial curved slot antenna with maximum bandwidth of 99.7% (2.2–6.6 GHz) for rectangular ($N = \infty$) shape is proposed. In [13], an elliptical patch is replaced with equivalent stepped edge polygon. Gain of the proposed antenna is not discussed in [13].

In this paper, a novel CPW-fed egg curved slot antenna with similar egg curved tuning stub is proposed. The measured results indicate that it has an extremely wide bandwidth of 1.95–20.0 GHz with consistent radiation patterns. It has a stable and relatively high gain of 4.1–5.1 dBi over 3.1–16.0 GHz. The proposed antenna can support many wireless services including WLAN (2.5 or 5–6 GHz) and UWB (3.1–10.6 GHz).

The paper is organised as follows. In Section 2, the proposed antenna geometry is described. In Section 3, several key parametric studies are performed for antenna optimisation and the bandwidth of various egg curved slot antennas has been discussed as the antenna design guideline. In Section 4, egg curved slot antennas with various structures are designed, fabricated and measured. Section 5 presents the conclusion.

2. ANTENNA CONFIGURATION

The CPW-fed printed egg curved slot antenna geometry and fabricated prototype are shown in Fig. 1(a) and Fig. 1(b) respectively. The proposed antenna of size $L_g \times W_g$ is etched on FR4 substrate with a relative permittivity ϵ_r (4.4) and height h (1.6 mm). Since the antenna is realized with coplanar technology, all the metal (copper) is removed from one side of the substrate. On the metallic side, it consists of a wide slot, a tuning stub and a 50 Ω CPW feed line of width W_f as shown in Fig. 1(a). The egg shape of proposed egg curved slot antenna (ECSA) is generated through egg shaping parameter k. The dimensions of the slot and stub are denoted as $L_s \times W_s$ and $L_t \times W_t$ respectively. The egg curved stub size and slot size are related by stub-to-slot size-ratio r.

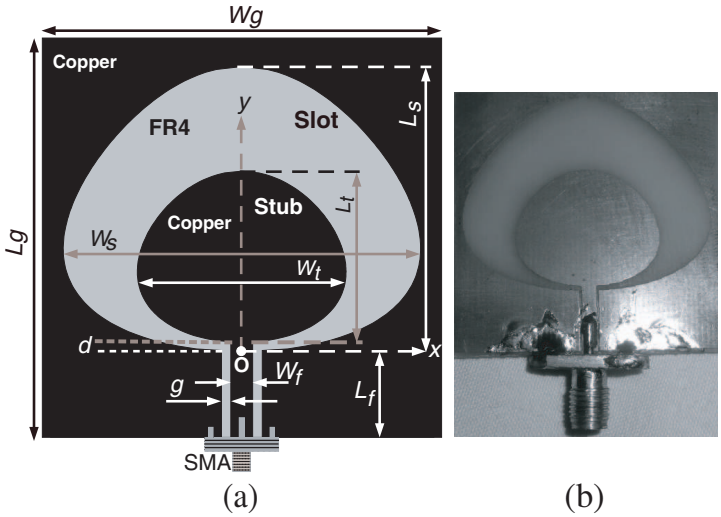

Figure 1. Proposed egg curved slot antenna (ECSA3: $k = 40$, $r = 0.6$). (a) Antenna geometry. (b) Fabricated prototype (FR4 based).

2.1. Generation of Egg Shape

The egg curve is obtained from the standard equation of an ellipse as follows:

$$\left[\frac{y}{b}\right]^2 + \left[\frac{x}{a}\right]^2 p(y) = 1 \tag{1}$$

where $p(y) = e^{ky}$, k = egg shaping parameter.

Different variations of egg shapes are obtained for various values of k and r as shown in Fig. 2. An ellipse is obtained for $k = 0$ as indicated in Fig. 2(a).

(a) ECSA1 (b) ECSA2 (c) ECSA4

Figure 2. Various ECSA configurations. (a) ECSA1: $k = 0$ (ellipse), $r = 0.6$. (b) ECSA2: $k = 20$, $r = 0.6$. (c) ECSA4: $k = 40$, $r = 0.3$.

2.2. Design of Egg Curved Slot and Stub

The egg curved slot is designed by using egg curve Equation (1) as follows:

$$\left[\frac{2y}{L_s}\right]^2 + \left[\frac{2x}{W_s}\right]^2 e^{ky} = 1 \tag{2}$$

A half of the egg shape is obtained from Equation (2) and then mirrored about y-axis. Thus a full egg shape is obtained. Then it is moved along y-axis by a distance L_f as shown in Fig. 1. The egg curved slot is excited by a $50\,\Omega$ CPW feed line. To achieve an efficient excitation and a wideband impedance matching [8, 12], the central signal strip is terminated to a similar egg curved tuning stub separated by an offset feedgap distance d from the slot as shown in Fig. 1. The stub-to-slot's outline size-ratio is denoted by parameter r as:

$$r = \frac{L_t}{L_s} = \frac{W_t}{W_s} \tag{3}$$

The egg curve function for the edge of the tuning stub can be written as follows:

$$\left[\frac{2y}{L_t}\right]^2 + \left[\frac{2x}{W_t}\right]^2 e^{ky} = 1 \tag{4}$$

Equation (4) may be rewritten using Equation (3) as:

$$\left[\frac{2y}{rL_s}\right]^2 + \left[\frac{2x}{rW_s}\right]^2 e^{ky} = 1 \tag{5}$$

After egg curved stub by Equation (5) is designed, it is moved along y-axis by distance $L_f + d$. The dissimilar shapes for tuning stub and slot structure may be generated with different values of egg shaping parameter k in egg curve Equations (2) and (5).

3. PARAMETRIC STUDY AND BW COMPARISON

In this section, the effect of ground plane size $L_g \times W_g$ and egg curved slot size $L_s \times W_s$ on impedance matching is analysed first. Then, the antenna bandwidths for various values of egg shaping parameter k and stub-to-slot size ratio r are compared and discussed. The simulation is carried out by using the 3-D full-wave electromagnetic simulation software Ansoft HFSS version 13.0.

3.1. Effect of Ground Size

The proposed egg curved slot antenna is simulated with different ground sizes to analyse the effect of ground plane dimensions on the antenna performance. The simulated reflection coefficient S_{11} for various ground size ($L_g \times W_g$) is plotted in Fig. 3. When ground width W_g decreases from 50 to 40 mm for ground size G_1 and G_0, the matching at the lower resonant frequency improves from 2.25 to 1.91 GHz correspondingly as shown in Fig. 3. Similarly, when ground length L_g increases from 40 to 50 mm for ground size G_1 and G_3, the matching at the lower resonant frequency improves from 2.25 to 1.90 GHz correspondingly. When the overall ground size ($L_g \times W_g$) is changed from $40 \times 40\,\text{mm}^2(G_0)$ to $45 \times 45\,\text{mm}^2(G_2)$ and $50 \times 50\,\text{mm}^2(G_3)$, the minor variation on the lower resonant frequency is observed as shown in Fig. 3. So a small ground size of $40 \times 40\,\text{mm}^2$ is selected as antenna size.

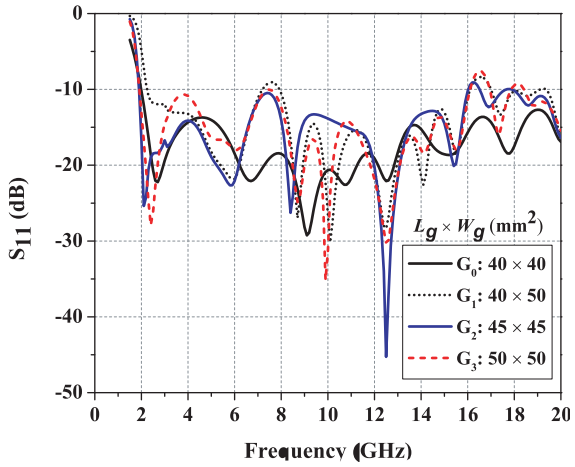

Figure 3. Simulated reflection coefficient S_{11} of proposed ECSA for various ground sizes ($L_s \times W_s = 30 \times 36\,\text{mm}^2$, $\epsilon_r = 4.4$, $W_f = 2.3\,\text{mm}$, $g = 0.25\,\text{mm}$, $L_f = 9\,\text{mm}$, $h = 1.6\,\text{mm}$, $r = 0.6$, $d = 0.6\,\text{mm}$, $k = 40$).

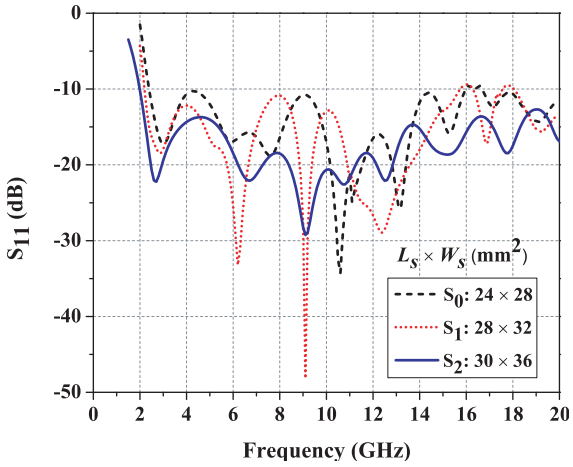

Figure 4. Simulated reflection coefficient S_{11} of proposed ECSA for various slot sizes ($L_g \times W_g = 40 \times 40\,\text{mm}^2$, $\epsilon_r = 4.4$, $W_f = 2.3\,\text{mm}$, $g = 0.25\,\text{mm}$, $L_f = 9\,\text{mm}$, $h = 1.6\,\text{mm}$, $r = 0.6$, $d = 0.6\,\text{mm}$, $k = 40$).

3.2. Effect of Slot Size

To attain an insight on the effect of slot geometry on the antenna performance, the proposed egg curved slot antennas are designed with different slot sizes as simulated in Fig. 4 and tabulated in Table 1. Over 155% bandwidth is observed for all the antennas and the operating frequencies are lowered as the size of the slot is increased.

Table 1. ($|S_{11}| \leq -10\,\text{dB}$) for various egg curved slot sizes ($L_g \times W_g = 40 \times 40\,\text{mm}^2$, $\epsilon_r = 4.4$, $W_f = 2.3\,\text{mm}$, $g = 0.25\,\text{mm}$, $L_f = 9\,\text{mm}$, $h = 1.6\,\text{mm}$, $r = 0.6$, $d = 0.6\,\text{mm}$, $k = 40$).

No.	Slot size $L_s \times W_s$ (mm^2)	Compu. f_L (GHz)	Simul. f_L (GHz)	Error (%)	%BW, Freq. range (for $\lvert S_{11}\rvert \leq -10\,\text{dB}$) (GHz)
S_0	24×28	2.28	2.36	3.4	157.78, 2.36–20.0
S_1	28×32	1.96	2.10	6.7	161.99, 2.10–20.0
S_2	30×36	1.81	1.91	5.2	165.13, 1.91–20.0

3.2.1. Determination of Lower Edge Frequency for $|S_{11}| \leq -10\,dB$

The proposed egg curved slot antenna ECSA4 ($k = 40$, $r = 0.6$) is obtained from standard elliptical ($k = 0$, $r = 0.6$) curve as discussed in previous section. Thus, the proposed antenna structure is a variation of the planar disc monopole antenna [9, 14]. The lower resonant frequency corresponding to $|S_{11}| \leq -10\,\text{dB}$ for printed egg curved slot antenna is given as [14, 15]:

$$f_L = \frac{7.2}{\kappa(L_s + 0.125W_s)} \tag{6}$$

Here, the value of κ is taken as 1.15 empirically for a dielectric layer with $\epsilon_r = 4.4$ and $h = 1.6\,\text{mm}$ [15]. The comparison between the computed and simulated values of the lower cut-off frequency of $-10\,\text{dB}$ operational bandwidth for different dimensions of egg curved slots is indicated in Table 1, and the corresponding simulated reflection coefficients for different dimensions of egg curved slot are plotted in Fig. 4. A maximum of 6.7% error (for slot size S_1) is observed between simulated and computed values of the lower cut-off frequency as mentioned in Table 1. This shows good match between simulated and computed values of the lower cut-off frequency of $-10\,\text{dB}$ operational bandwidth for proposed ECSA.

3.3. Egg Shaping Parameter *k*

The measured and simulated reflection coefficients for different values of egg shaping parameter k are plotted in the Fig. 5 to study the effect of egg curved slot geometry on impedance bandwidth. The bandwidth comparison of proposed ECSAs for varoius values of k and r is indicated in Table 2. When egg shaping parameter k is varied from 0 (ECSA1) to 40 (ECSA3), the simulated lower resonant frequency (for $|S_{11}| \leq -10\,\text{dB}$) of the egg curved slot antenna decreases from 3.75 to 1.91 GHz correspondingly, as mentioned in Table 2. Thus a wide simulation bandwidth of 165.13% is obtained for proposed ECSA3 as compared to 136.84% bandwidth of ECSA1. It is clear from Table 2 that the measured impedance bandwidths match well with the simulated ones. Table 2 also shows that all the egg curved slot antennas have obtained wide impedance bandwidth in excess of 135%. Fig. 5 also shows the comparison of simulated and measured reflection coefficients of proposed egg curved slot antennas with the binomial curved antennas proposed in [11, 12]. The simulated impedance bandwidth of proposed ECSA3 is 1.91–20.0 GHz for $|S_{11}| \leq -10\,\text{dB}$ which is considerably larger than the impedance bandwidth achieved by binomial curved slot antenna (2.45–5.29 GHz) [12] and planar binomial curved monopole antenna (2.71–10.70 GHz) [11]. Thus egg curved slot antennas offer very wide impedance bandwidth as compared to other curved antennas.

Table 2. Bandwidth comparison for various ECSAs ($L_g \times W_g = 40 \times 40\,\text{mm}^2$, $L_s \times W_s = 30 \times 36\,\text{mm}^2$, $\epsilon_r = 4.4$, $W_f = 2.3\,\text{mm}$, $g = 0.25\,\text{mm}$, $L_f = 9\,\text{mm}$, $h = 1.6\,\text{mm}$, $d = 0.6\,\text{mm}$).

Antennas	Design Param.		%BW ($\|S_{11}\| \leq -10\,\text{dB}$), Freq. range (GHz)	
	k	r	Simulated	Measured
ECSA1	0	0.6	136.84, 3.75–20.0	136.28, 3.79–20.0
ECSA2	20	0.6	163.64, 2.0–20.0	161.17, 2.15–20.0
ECSA3	40	0.6	165.13, 1.91–20.0	164.46, 1.95–20.0
ECSA4	40	0.3	140.43, 3.50–20.0	138.46, 3.60–19.8
ECSA5	40	0.4	153.67, 2.62–20.0	–
ECSA6	40	0.5	160.04, 2.22–20.0	–

3.4. Stub-Slot Size Ratio *r*

The impedance bandwidth is limited by matching between the feed stub shape and the wide slot on the ground plane. It is found that good impedance matching can be obtained by enhancing the coupling

between the slot and the feed stub. In order to achieve a high level of electromagnetic coupling to the feed line, a large slot is used in a wide egg curved slot antenna and its dimensions are optimized. This effect is studied through variation in stub-to-slot size ratio r as shown in Table 2. Fig. 6 shows the comparison between the simulated reflection coefficients for various values of r. When the coupling is increased with $r = 0.3$ (ECSA4) to 0.6 (ECSA3), the simulated lower resonant frequency for $|S_{11}| \leq -10$ dB is reduced from 3.50 to 1.91 GHz correspondingly, while upper frequency limit is still maintained at 20 GHz as mentioned in Table 2. Thus the simulation bandwidth of ECSAs increased from 140.43% (ECSA4) to 165.13% (ECSA3) through the variation in stub-to-slot size ratio r. However, the impedance matching is deteriorated with further increase in the coupling. Therefore, varying the feed stub shape or slot shape will change the coupling property and consequently the operating bandwidth. On the other hand, for optimum performance, the feed stub and slot shapes should be similar and the feed stub should occupy an area of about 60% of the slot size. Thus, an optimum measured bandwidth of 1.95–20.0 GHz is obtained for $r = 0.6$.

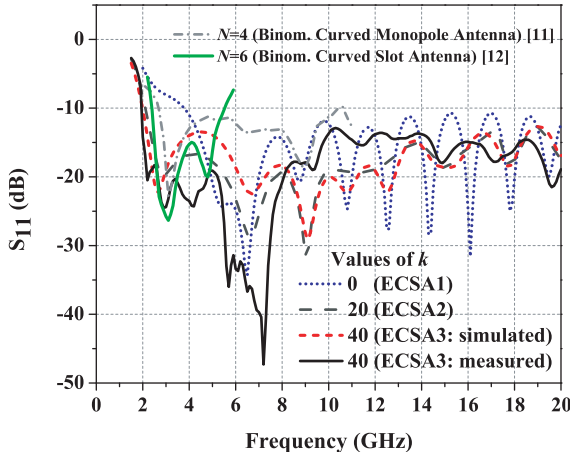

Figure 5. Comparison of simulated and measured reflection coefficients S_{11} for various values of egg shaping parameter k with binomial curved antennas.

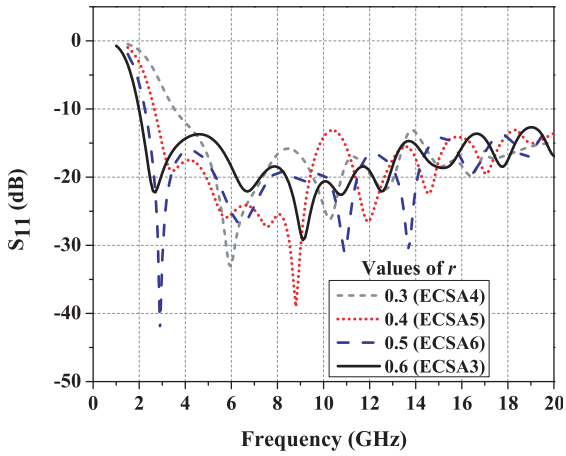

Figure 6. Simulated reflection coefficient S_{11} for various values of stub-to-slot size ratio r.

3.5. Offset Feed Gap Parameter *d*

The offset feed gap parameter d determines the matching between the feed line and the wide egg curved slot antenna as it acts as a matching network. It is observed that good impedance matching can be obtained by enhancing the coupling between the slot and the feed. Fig. 7 plots simulated reflection coefficient for various values of d. It can be observed that the lower cut-off frequency of -10 dB impedance bandwidth is clearly independent of the feed gap but upper cut-off frequency is dependent on it. An optimum impedance matching is obtained for $d = 0.6$ mm.

4. RESULTS AND DISCUSSION

The proposed egg curved wide-slot antennas were initially simulated and then, fabricated and measured. The antenna measurements have been obtained with an Agilent E5071C ENA Network Analyzer in its full operational scan (1–20 GHz). Fig. 5 shows that the proposed antenna ECSA3 has achieved measured impedance bandwidth of 1.95–20.0 GHz. In this section, experimental and simulation results are presented.

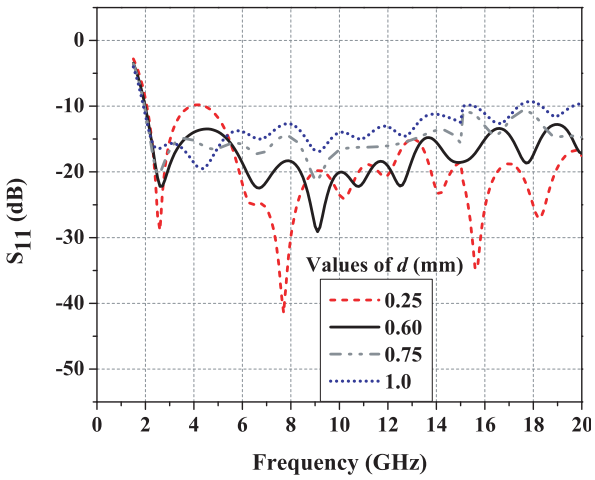

Figure 7. Simulated reflection coefficient S_{11} for various values of offset gap parameter d ($L_g \times W_g = 40 \times 40\,\text{mm}^2$, $L_s \times W_s = 30 \times 36\,\text{mm}^2$, $\epsilon_r = 4.4$, $W_f = 2.3\,\text{mm}$, $g = 0.25\,\text{mm}$, $L_f = 9\,\text{mm}$, $h = 1.6\,\text{mm}$, $r = 0.6$, $k = 40$).

4.1. Current Distribution

The generation of resonant modes is strongly dependent on the shape and size of the radiator [16]. The simulated surface current distributions of the proposed ECSAs for different shape and size, obtained by changing the values of egg shaping parameter k and stub-slot size ratio r are shown at different frequencies in Fig. 8. It is obvious from Fig. 8(a) that ECSA3 ($k = 40$, $r = 0.6$) operates in fundamental mode of operation at 2.6 GHz with similar current distribution like that of wire monopole of quarter wavelength [9]. The direction of the current is almost vertically upward in the stub and the ground plane with no null because it operates in oscillating mode at 2.6 GHz and as a result, standing wave is formed. At higher mode (6.4 GHz), the direction of the current is almost vertically downward in the stub, while currents are in the opposite direction around the edge of the egg curved slot as shown in Fig. 8(b). As the frequency is further increased to 12.5 and 17.8 GHz as shown in Fig. 8(c) and Fig. 8(d) respectively, the number of nulls increases and the current appears to move in opposite direction at the edge of the egg curved slot which shows that the traveling waves are dominant at higher frequencies. It is important to note that the wavelengths at these frequencies are smaller than the antenna structure. When the shape of the proposed egg curved slot antenna structure is changed from egg shape (ECSA3: $k = 40$, $r = 0.6$) to elliptical shape (ECSA1: $k = 0$, $r = 0.6$) or stub-slot size ratio r is reduced from 0.6 (ECSA3: $k = 40$, $r = 0.6$) to 0.3 (ECSA4: $k = 40$, $r = 0.3$), the corresponding simulated current distributions of ECSA1 and ECSA4 are shown in Fig. 8(e) and Fig. 8(f) respectively. It is clear from Fig. 8(e) and Fig. 8(f) that the currents move in opposite directions with nulls in case of both the antennas ECSA1 and ECSA4 at their first resonant mode frequencies 6.2 GHz and 6.0 GHz respectively. Hence, both of these antennas operate in traveling waves modes only. Therefore, the impedance bandwidths of ECSA1 and ECSA4 are lesser than the bandwidth of ECSA3 as indicated in Table 2 also. Further, it is also observed from Fig. 5 that the proposed egg curved slot antennas are capable of supporting multiple resonant modes and the overlapping of all of these resonant modes leads to their wideband characteristics, while only two resonant modes were obtained at 3.0 GHz and 4.7 GHz frequencies for binomial curved slot antenna ($N = 6$) which resulted in its smaller bandwidth [12].

4.2. Radiation Patterns

The simulated and measured far-field E-plane (or yz-plane) and H-plane (or xz-plane) normalized radiation patterns of the proposed egg curved slot antenna ECSA3 at the several typical frequencies are presented in Fig. 9. The copolarised components in the E-plane (or yz-plane) and H-plane (or xz-plane) are E_θ and E_ϕ, respectively. The experimental results show good agreement with the simulation results. It can be observed that the proposed antenna has almost the same normalized radiation patterns over the

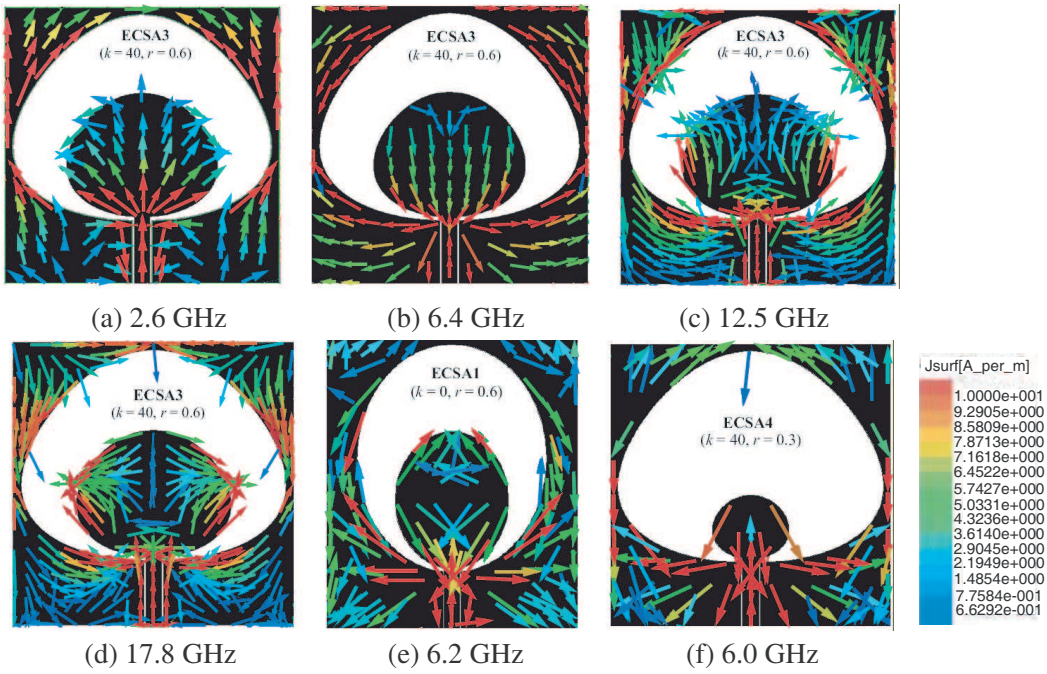

Figure 8. Simulated current distributions of proposed egg curved slot antennas at different frequencies.

entire antenna bandwidth. Specifically, they show symmetrical and omnidirectional radiation patterns in H-planes, whereas bidirectional in the E-planes. These patterns also show that the proposed antennas provide good cross polar discrimination over entire antenna bandwidth. The copolar to crosspolar ratio of more than 30 dB is observed at boresight in all the measured radiation patterns.

The simulated 3D radiation patterns of the proposed ECSA3 at 2.4, 3.5, 9 and 20 GHz are also shown in the Figs. 9(c), 9(f), 9(i) and 9(l), respectively. In 3D patterns, the red colour indicates the strongest radiation and the blue colour is for the weakest ones. The radiation pattern looks like a doughnut, similar to that of a dipole pattern, at the lower frequencies i.e., 2.4 and 3.5 GHz. At higher frequency 9 GHz, the radiation pattern is somewhat like pinched doughnut (i.e., omnidirectional in H-plane). As the frequency moves toward the upper end of the bandwidth i.e., at 20 GHz, the radiation pattern is some what slightly distorted due to higher order harmonics. The transition of the 3D-radiation patterns from a simple doughnut at the lower frequencies to the complicated 3D-radiation patterns at the higher resonances indicates that this antenna must have gone through major changes in its behavior but it had retained its omnidirectional behaviour in H-plane. Hence, the radiation patterns of the proposed antenna are acceptable for ultrawideband and many existing wireless services.

4.3. Gain

Good match between measured and simulated realised gain of proposed ECSA3 in the boresight direction across the entire frequency band is shown in Fig. 10. Table 3 shows the comparison of realised gain variations of proposed ECSA3 with other curved antennas [11, 12] over various frequency intervals. The realised gain for proposed ECSA3 is measured as 4.1–5.1 dBi over 3.1–16.0 GHz with gain variation of 1.0 dBi and 4.8–5.4 dBi over 16.1–20.0 GHz as mentioned in Table 3. Thus proposed ECSA3 shows relatively high and stable gain with less gain variation as compared to antennas stated in [11, 12]. Though elliptical monopole antenna with modified feed [4] of relatively larger size $110 \times 124\,\text{mm}^2$ has a wide impedance bandwidth but it has a large gain variation of approximately 6.5 dBi over its entire antenna bandwidth (1.0–20.0 GHz). The gain stability of the proposed ECSA3 also indicates the consistency of its radiation patterns over the entire antenna bandwidth.

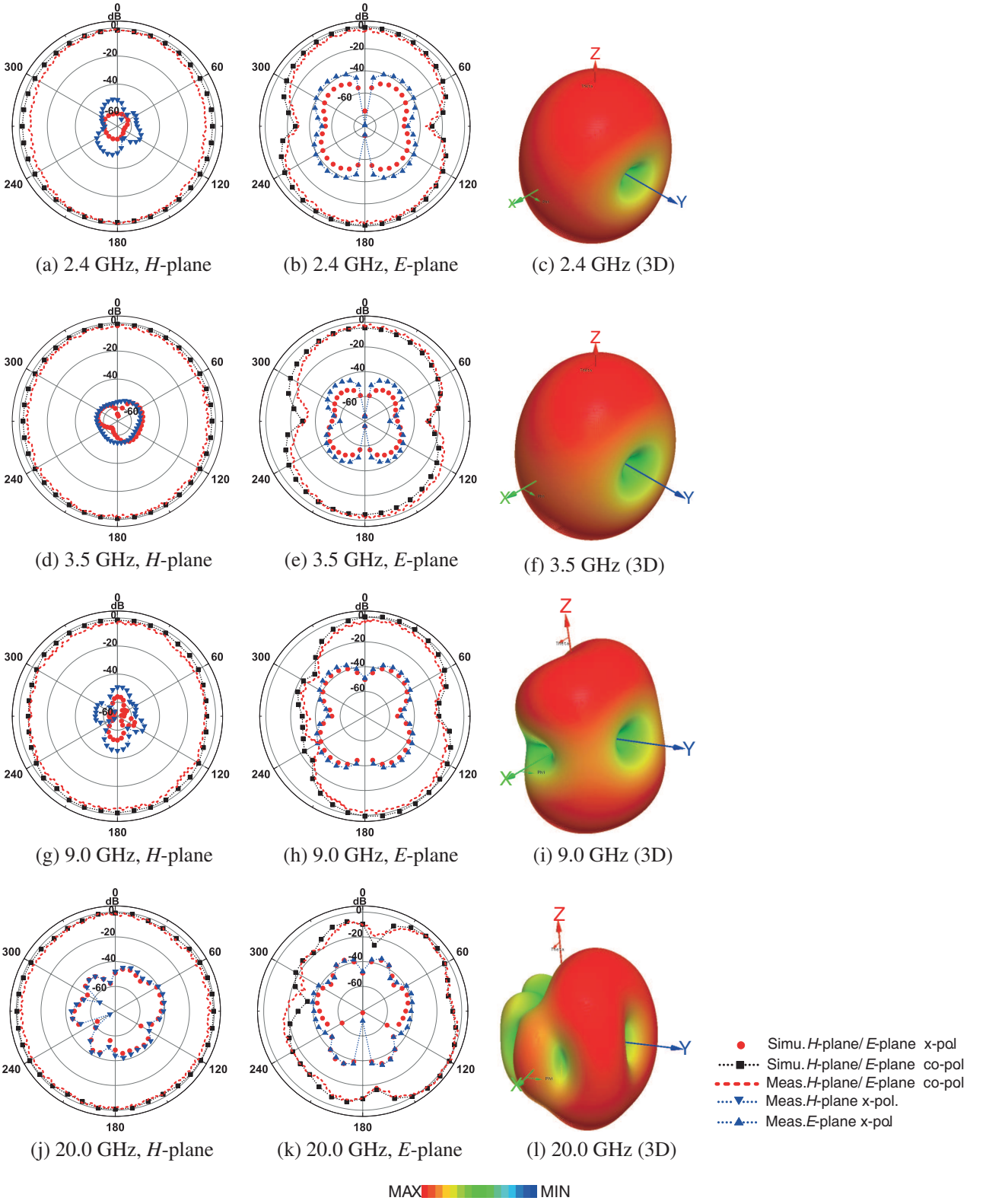

(a) 2.4 GHz, *H*-plane (b) 2.4 GHz, *E*-plane (c) 2.4 GHz (3D)

(d) 3.5 GHz, *H*-plane (e) 3.5 GHz, *E*-plane (f) 3.5 GHz (3D)

(g) 9.0 GHz, *H*-plane (h) 9.0 GHz, *E*-plane (i) 9.0 GHz (3D)

(j) 20.0 GHz, *H*-plane (k) 20.0 GHz, *E*-plane (l) 20.0 GHz (3D)

Figure 9. Comparison between simulated and measured normalized 2D-radiation patterns along with simulated 3D-radiation patterns of proposed ECSA3.

Table 3. Performance comparison of various printed curved antennas.

Antenna Config.	Patch Dim. $L_g \times W_g$ (mm^2)	Simul. BW ($\lvert S_{11}\rvert \leq -10$ dB) %, (GHz)	Simul. realised gain Frequency range (dBi), (GHz)	Meas. realised gain Frequency range (dBi), (GHz)
Egg curved slot ant. (ECSA3)	40×40	165.13, 1.91–20.0	2.7–4.2, 1.95–3.0 4.3–5.6, 3.1–16.0 5.5–6.2, 16.1–20.0	2.7–4.0, 1.95–3.0 4.1–5.1, 3.1–16.0 4.8–5.4, 16.1–20.0
Binomial curved slot ant. ($N = 6$) [12]	35×40	73.39, 2.45–5.29	3.5–4.8, 2.45–5.29	–
Binomial curved monopole ($N = 4$) [11]	70×46	119.16, 2.71–10.70	–	−0.88–1.54, 3.1–11.0

5. CONCLUSION

Printed egg curved slot antennas with CPW-feed of size $40 \times 40\,mm^2$ are proposed and designed by introducing an egg shaping parameter in standard elliptic curve to generate egg shape from ellipse. Numerical simulations have been validated experimentally, and good agreement was obtained. An empirical formula is proposed to approximately determine the lower edge frequency of $\lvert S_{11}\rvert \leq -10$ dB operating bandwidth. The bandwidth of proposed antenna is measured as 164.46% (from 1.95 to 20.0 GHz). Moreover, by different stub-to-slot size ratio and feed gap spacing, various antennas with different bandwidths are also obtained. In addition to smaller size, the proposed antenna provides stable and almost omnidirectional radiation patterns in H-plane, low crosspolar radiation and relatively high and nearly flat gains over the entire operating bandwidth. All these features make the proposed design a suitable choice for emerging ultrawideband and wideband applications.

REFERENCES

1. Jan, J.-Y. and J.-W. Su, "Bandwidth enhancement of a printed wide-slot antenna with a rotated slot," *IEEE Trans. Antennas Propag.*, Vol. 53, No. 6, 2111–2114, 2005.
2. Jan, J.-Y. and L.-C. Wang, "Printed wideband rhombus slot antenna with a pair of parasitic strips for multiband applications," *IEEE Trans. Antennas Propag.*, Vol. 57, No. 4, 1267–1270, 2009.
3. Tsai, C.-L. and C.-L. Yang, "Novel compact eye-shaped UWB antennas," *IEEE Antennas Wireless Propag. Lett.*, Vol. 11, 184–187, 2012.
4. Liu, J., S. Zhong, and K. Esselle, "A printed elliptical monopole antenna with modified feeding structure for bandwidth enhancement," *IEEE Trans. Antennas Propag.*, Vol. 59, No. 2, 667–670, 2011.
5. Chiou, J.-Y., J.-Y. Sze, and K.-L. Wong, "A broad-band CPW-fed striploaded square slot antenna," *IEEE Trans. Antennas Propag.*, Vol. 51, No. 4, 719–721, 2003.
6. Denidni, T. and M. Habib, "Broadband printed CPW-fed circular slot antenna," *Electron. Lett.*, Vol. 42, No. 3, 135–136, 2006.
7. Krishna, D., M. Gopikrishna, C. Anandan, P. Mohanan, and K. Vasudevan, "CPW-fed koch fractal slot antenna for WLAN/WiMAX applications," *IEEE Antennas Wireless Propag. Lett.*, Vol. 7, 389–392, 2008.
8. Dastranj, A. and H. Abiri, "Bandwidth enhancement of printed E-Shaped slot antennas fed by CPW and microstrip line," *IEEE Trans. Antennas Propag.*, Vol. 58, No. 4, 1402–1407, 2010.
9. Li, P., J. Liang, and X. Chen, "Study of printed elliptical/circular slot antennas for ultrawideband applications," *IEEE Trans. Antennas Propag.*, Vol. 54, No. 6, 1670–1675, 2006.

10. Ma, T.-G. and C.-H. Tseng, "An ultrawideband coplanar waveguide-fed tapered ring slot antenna," *IEEE Trans. Antennas Propag.*, Vol. 54, No. 4, 1105–1110, 2006.
11. Ling, C.-W., W.-H. Lo, R.-H. Yan, and S.-J. Chung, "Planar binomial curved monopole antennas for ultrawideband communication," *IEEE Trans. Antennas Propag.*, Vol. 55, No. 9, 2622–2624, 2007.
12. Liang, C.-W., T. Denidni, L.-N. Zhang, R.-H. Jin, J.-P. Geng, and Q. Yu, "Printed binomial-curved slot antennas for various wideband applications," *IEEE Trans. Microw. Theory Tech.*, Vol. 59, No. 4, 1058–1065, 2011.
13. Sorokosz, L. and W. Zieniutycz, "On the approximation of the UWB dipole elliptical arms with stepped-edge polygon," *IEEE Antennas Wireless Propag. Lett.*, Vol. 11, 636–639, 2012.
14. Kumar, G. and K. P. Ray, *Broadband Microstrip Antennas*, Artech House, Norwood, MA, 2003.
15. Ray, K. and Y. Ranga, "Ultrawideband printed elliptical monopole antennas," *IEEE Trans. Antennas Propag.*, Vol. 55, No. 4, 1189–1192, 2007.
16. Wu, W. and Y.-P. Zhang, "Analysis of ultra-wideband printed planar quasi-monopole antennas using the theory of characteristic modes," *IEEE Antennas Propag. Mag.*, Vol. 52, No. 6, 67–77, 2010.